Towards violations of Local Friendliness with quantum computers

William J. Zeng[1,2], Farrokh Labib[1], and Vincent Russo[1]

[1]Unitary Foundation
[2]Quantonation

Local Friendliness (LF) inequalities follow from seemingly reasonable assumptions about reality: (i) "absoluteness of observed events" (e.g., every observed event happens for all observers) and (ii) "local agency" (e.g., free choices can be made uncorrelated with other events outside their future light cone). Extended Wigner's Friend Scenario (EWFS) thought experiments show that textbook quantum mechanics violates these inequalities. Thus, experimental evidence of these violations would make these two assumptions incompatible. In [Nature Physics 16, 1199 (2020)], the authors experimentally implemented an EWFS, using a photonic qubit to play the role of each of the "friends" and measured violations of LF. One may question whether a photonic qubit is a physical system that counts as an "observer" and thereby question whether the experiment's outcome is significant. Intending to measure increasingly meaningful violations, we propose using a statistical measure called the "branch factor" to quantify the "observerness" of the system. We then encode the EWFS as a quantum circuit such that the components of the circuit that define the friend are quantum systems of increasing branch factor. We run this circuit on quantum simulators and hardware devices, observing LF violations as the system sizes scale. As errors in quantum computers reduce the significance of the violations, better quantum computers can produce better violations. Our results extend the state of the art in proof-of-concept experimental violations from branch factor 0.0 to branch factor 16.0. This is an initial result in an experimental program for measuring LF violations at increasingly meaningful branch factors using increasingly more powerful quantum processors and networks. We introduce this program as a fundamental science application for near-term and developing quantum technology.

1 Introduction

Experimental quantum mechanics has long produced evidence that reality differs from what naive human intuition expects. These experimental results sometimes go beyond supporting specific quantum mechanical predictions and give evidence against whole classes of physical theories that obey certain principles. For example, experimental violations of Bell inequalities provide evidence for quantum mechanics and show that reality is not described by any theories (even super-quantum ones) that maintain both local agency and local hidden variables. These results are part of *experimental metaphysics* [1, 2], giving evidence about possible physical theories at the *meta* level.

William J. Zeng: will@unitary.foundation.com, https://willzeng.com/
Farrokh Labib: farrokh@unitary.foundation
Vincent Russo: vincent@unitary.foundation, https://vprusso.github.io/

New tests in experimental metaphysics have been proposed to study the metaphysical property of *Local Friendliness* (LF) [3]. Local Friendliness (defined more formally in Section 2) is loosely the conjunction of *objective reality across observers* and *local agency*. Thus, a violation of the Local Friendliness property provides evidence that one of these two assumptions need to be jettisoned. Local Friendliness tests are formalizations and extensions of the Wigner's Friend thought experiment from the 1960's [4]. In this work, we:

1. propose how quantum computers (and related quantum technology like quantum networks) can be used to build increasingly more meaningful (larger and loophole-free) tests of Local Friendliness and

2. use small quantum computers to give experimental evidence (with loopholes) of Local Friendliness violations as a first step in this program.

The improvement of quantum technology through academic and industrial development opens up new avenues for studying fundamental scientific questions. We are optimistic that a program of Local Friendliness violations can motivate continued development and benchmarking of quantum technology by testing important aspects of reality.

This paper proceeds as follows: first, we introduce Local Friendliness inequalities and the Extended Wigner's Friend Scenario experiments that can be used to violate them. We then propose our experimental program for increasingly significant LF violations and focus on the branch factor as the measure of observerness. Next, we demonstrate violations of LF (with loopholes) at the highest branch factors yet observed by using quantum computers as an experimental platform. To do this, we introduce practical approaches to deal with noise in our experiments, including validating branch factors under noise and reducing the impact of measurement noise. Finally, we conclude with future directions for advancing the proposed experimental program.

2 Local Friendliness and tests to violate it

Local Friendliness comes from the conjunction of two basic assumptions about reality [3, 5]. We first introduce these assumptions as metaphysical principles and later define them in a particular experimental setup for testing Local Friendliness violations.

Definition 2.1 (Absoluteness of Observed Events (AOE)**.** *Every observed event happens for all observers.*

AOE states that if an event occurs, it does not occur relative to any particular observer. This can be viewed as a weaker condition than the intuition violated by standard relativity. Relativity tells us that two observers may disagree on the time an event occurs, whereas dropping the assumption of AOE means there could be a potential disagreement about whether an event occurred.

Definition 2.2 (Local Agency (LA))**.** *Free choices are uncorrelated with other events outside their future light cone.*

At a high level, LA can be interpreted to mean that one can construct independent variables. In other words, LA says that there are events that do not influence the probabilities of other events. We will need to be able to make these uncorrelated events in our particular experimental scenarios to show violations.[1]

Definition 2.3 (Local Friendliness (LF))**.** *The conjunction of AOE and LA.*

[1]Local Agency can be analyzed into separate assumptions of Interventionist Causation and a Relativistic Causal Arrow. See [6] and [7] for more details.

It turns out that thought experiments can be designed whereby textbook quantum mechanics violates the assumption of LF. These thought experiments build upon the Wigner's Friend thought experiment initially proposed by Wigner in [4] and later refined by Deutsch in [8]. The implications of these violations being experimentally confirmed are significant. One is forced to either:

- Drop AOE. This means that nature allows separate realities for different observers, called *Wigner bubbles* by Cavalcanti [9]. There are also other proposals for refuting AOE [10, 11, 12, 13, 14, 15, 16]. While we are accustomed to social and philosophical subjectivity, introducing this subjectivity into the heart of physics is a meaningful move.

- Drop LA. This would be consistent with nonlocal hidden variable theories or with some form of superdeterminism [17].

While different interpretations of quantum mechanics support keeping or dropping either LA or AOE, a meaningful LF violation means one *must* drop one to remain consistent. Alternatively, one should propose some rule for why one interpretation should be applied in one scenario and not others. Remaining generally "interpretation agnostic" would no longer be tenable.

2.1 Wigner's Friend and Extended Wigner's Friend Scenario thought experiments

The Wigner's Friend thought experiment (Figure 1) consists of an observer, Alice, and her friend, Charlie. We assume Charlie is in an isolated laboratory, receiving and measuring part of an entangled quantum system. Upon measurement, the outcome obtained by Charlie is known to him but is still not known to Alice (as she is outside of the isolated laboratory). Charlie then emerges from his laboratory to inform Alice of the result of Charlie's measurement. Before Alice receives this information, however, one could represent Alice's knowledge of the quantum system measured by Charlie as still in a superposition (even after Charlie has measured and collapsed the quantum system). It is only after Alice receives the measurement outcome information from Charlie that her superposition representation of the state prepared and measured by Charlie collapses to the same measurement outcome that Charlie previously obtained. If collapse is supposed to be an objective physical process, then this uncertainty is uncomfortable.

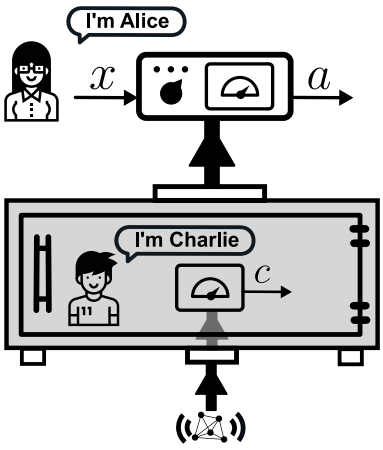

Figure 1: **Conceptual rendering of the Wigner's Friend scenario.** A system is sent into Charlie's sealed lab. Alice has different measurement settings labeled by x to observe the sealed lab that contains her friend Charlie and his measurement outcome c. Alice's measurement outcome has the value labeled a. Figure replicated and modified with permission from the authors from [3].

This original thought experiment highlights that it is unclear when the quantum system collapses (under a Copenhagen interpretation). From Charlie's perspective, the collapse happened

when he applied a measurement to his quantum system inside the isolated laboratory and obtained his measurement outcome. Alternatively, from Alice's perspective, the collapse occurred when Alice obtained information from Charlie about the measurement outcome he obtained.

Building on the original Wigner's Friend thought experiment, work by Brukner [18, 19] and by Frauchiger and Renner [20] led to an extension of the thought experiment called the *Extended Wigner's Friend Scenario* (EWFS), illustrated in Figure 2. One common framing of the extended Wigner's Friend Scenario comprises parallel instances of the original Wigner's Friend thought experiment [2]. We now consider two observers, Alice and Bob, and their respective friends, Charlie and Debbie. The friends are each contained in their respective isolated laboratories and possess some quantum system they share. They each carry out a measurement and subsequently relay these measurement outcomes to their observer counterparts.

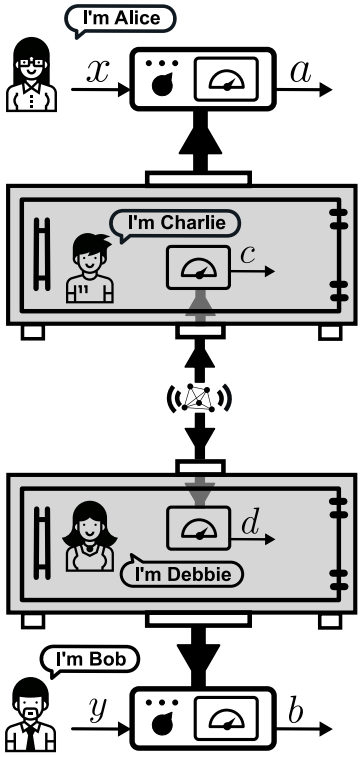

Figure 2: **Conceptual rendering of an Extended Wigner's Friend Scenario (EWFS).** A system is split and sent into two sealed labs. Alice has different measurement settings labeled by x to observe the sealed lab that contains her friend Charlie and his measurement outcome c. Similarly, Bob has measurement settings labeled by y for the sealed lab containing Debbie and her measurement outcome d. Alice's measurement outcome has the value labeled a, and Bob's has the value labeled b. Figure replicated with permission from the authors from [3].

In [3], the authors performed an experiment with a specific instance of the EWFS and derived specific LF inequalities that were experimentally violated. In principle, one could consider generalized extensions of the EWFS in which there are at least two observers and a corresponding number of associated friends. Examples of these multiparty scenarios and associated LF inequalities are studied in [24]. For our purposes, and the scenario presented in [20] and [3], we restrict our attention to the Extended Wigner's Friend Scenarios of two parties. We note that, for explanatory purposes, our description makes references to quantum theory, but the Local Friendliness inequalities are theory-independent.

[2]This framing of the EWFS is not the only one that others have considered. Indeed, there have been others based on the notion of contextuality [11, 21, 22]. We refer the reader to this review for other such setups for EWFS [23].

For the two-party EWFS, the friends Charlie and Debbie share a (not necessarily entangled) quantum system, where S_C is the part of the system in possession of Charlie and S_D is the system in possession of Debbie. Charlie and Debbie are each in isolated labs where they perform a measurement in some specified basis on their respective part of the system and record the outcome in, say, their memory. Define F_C as Charlie's laboratory, excluding the system S_C and similarly F_D for Debbie. Charlie's measurement of S_C (in some specified basis) is, according to the observer Alice, a unitary that acts on $\mathcal{H}_{F_C} \otimes \mathcal{H}_{S_C}$ where $\mathcal{H}_X$ is the Hilbert space associated to system X, similarly, for Bob and his friend Debbie.

From Alice and Bob's perspective, there are two ways that they can choose to measure the quantum system. They can open the lab and simply "peek" at the classical measurement outcome recorded by their friend in the lab. Alternatively, they can measure the quantum system themselves by reversing the measurement process that the friends performed, and then directly measuring the quantum system in a basis of their choosing. They can do this because the friend's measurement process is unitary, and we assume that Alice and Bob can manipulate the isolated labs in any way that quantum theory allows. Interestingly, it can be shown that no-signaling implies that the friends (Charlie and Debbie) are not only not aware of what outcome they had before being reversed, but also that they cannot be aware of having been reversed [25].

Unfortunately, performing this experiment with macroscopic observers as friends is beyond what we could imagine engineering. Instead, we model each friend (Charlie and Debbie) as a system of qubits. We model measurements performed by the friends as a CNOT gate. For example, if Charlie measures S_C, we apply a CNOT controlled from S_C to the qubit(s) modeling Charlie. From Alice's perspective, the measurement is a unitary operation that she can reverse. In the following section, we illustrate how this produces a violation of Local Friendliness.

2.2 Quantum mechanical violations of LF in the three-setting two-party EWFS

In this section, we consider the specific details of the two-party and three-setting EWFS experimentally carried out in [3]. A conceptual diagram is given in Figure 2. Following the EWFS described in [3], we consider two observers, Alice and Bob, who have the option of choosing amongst three possible measurement settings labeled as $x, y \in \{1, 2, 3\}$ where x is Alice's setting and y is Bob's setting. Alice and Bob have respective friends, Charlie and Debbie, who share some bipartite quantum system and must measure their share of the system in a basis that depends on the x and y settings, respectively.

If Alice chooses $x = 1$, she peeks and measures Charlie directly (in the computational basis). If Alice selects $x = 2$ or $x = 3$, she reverses the measurement operation performed by Charlie and measures the system in a basis that depends on x. The same procedure holds for Bob and his friend Debbie, but possibly with different basis measurements. To clarify the measurement setting labels, we will use the convention that $x = 1$ or $y = 1$ is the PEEK setting and $x \in \{2, 3\}$ or $y \in \{2, 3\}$ are the REVERSE-1 and REVERSE-2 settings, respectively.

We can implement the EWFS in a quantum circuit (an example is shown in Figure 7). We are interested in the expectation values of observables on the subsets of qubits of these quantum circuits that represent the outcomes for Alice and Bob. We implement the EWFS in a quantum circuit where we can only do measurements in the computational basis. So, implementing a measurement in a rotated basis is achieved by simply applying some rotation gates before measuring in the computational basis. Hence, the chosen settings x and y determine what circuit to run.

LF inequalities bound what observed outcome statistics are possible for Alice and Bob when LF holds [3]. For measurement settings $x, y \in \{1, 2, 3\} = \{\text{PEEK, REVERSE-1, REVERSE-2}\}$, we denote A_x and B_y as the corresponding observables for Alice and Bob. We note that before being derived in [3], the LF inequalities were obtained under a different context regarding device-independent settings [26, 27, 28] in this thesis [29] (Appendix-A) under the name of "partially deterministic polytopes". Situated between the local and no-signaling polytopes, these partially

deterministic polytopes define the boundaries of behaviors for which randomness certification is impossible against a no-signaling adversary, given a specific set of measurements. They serve as a bridge, connecting the extremes of local and no-signaling constraints in the landscape of quantum behaviors. This connection was also pointed out in [3] and has been subsequently investigated in [24].

Quantum mechanics indicates that it should, in principle, be possible to violate these LF inequalities. In [3], the authors considered a specific bipartite state and sets of measurements for Alice and Bob that violated each of the LF inequalities in their work. Our work is exclusively focused on the so-called *semi-Brukner* inequality which is defined as:

$$-\langle A_1 B_2\rangle + \langle A_1 B_3\rangle - \langle A_3 B_2\rangle - \langle A_3 B_3\rangle - 2 \leq 0. \tag{1}$$

We reproduce the specific strategy in [3] that violates these inequalities. Let $|\psi\rangle \in \mathcal{H}_{S_C} \otimes \mathcal{H}_{S_D}$ be the entangled quantum state held by Charlie and Debbie is defined as

$$\frac{1}{\sqrt{2}}\left(|01\rangle - |10\rangle\right) \in \mathcal{H}_{S_C} \otimes \mathcal{H}_{S_D}. \tag{2}$$

Additionally, define the projectors $\Pi_\theta^\pm = |\phi_\theta^\pm\rangle\langle\phi_\theta^\pm|$ parameterized by an angle $\theta \in [0, 2\pi]$ where

$$\left|\phi_\theta^\pm\right\rangle = \frac{1}{\sqrt{2}}\left(|0\rangle \pm e^{i\theta}\,|1\rangle\right). \tag{3}$$

Define the observable

$$O_\theta = \Pi_\theta^+ - \Pi_\theta^-. \tag{4}$$

In the middle column of Table 1, the upper bound on the left-hand side of the semi-Brukner inequality is reported using the angles as described in [3], while in the right column, the maximum possible violation is reported by optimizing over the possible angles θ.

Inequality	LHS of inequality w/ [3] setup	LHS of inequality w/ the optimal angles (Sec. 4)
Semi-Brukner	0.380364	0.82843

Table 1: Middle Column: The theoretical results from [3] for the left-hand sides of the semi-Brukner inequality. Right Column: The theoretical maximum for the left-hand sides of the inequality when we choose the optimal strategy as described in Sec. 4.

2.3 EWFS scenarios with one friend

Notice that there is no PEEK setting for Bob in the semi-Brukner inequality, so he never applies a direct measurement to Debbie, but only measures the system qubit. In fact, we can show that the semi-Brukner inequality still holds even when we remove Debbie from the scenario entirely. We prove this statement in this section. This simplification significantly reduces the resources required to implement the scenario.

We consider the EWFS scenario where only Alice has a friend (Charlie) while Bob is on his own. The two parties still share an entangled state on which they apply their respective measurements. Only Alice has the ability to peek in her lab and see what her friend measured or reverse the measurement performed by Charlie. This single-friend EWFS variant is depicted in Figure 3.

The assumptions on the probability distribution that give the correlations on their outcomes should satisfy AOE and LA. [3]. Let $\phi(ab|xy)$ be the distribution of Alice and Bob's outcomes a, b given their measurement choices x, y. AOE and LA apply constraints on the distribution of all measurement outcomes $P(abcd|xy)$ given those measurement choices.

[3]Local Agency is the conjunction of No Superdeterminism and Locality in [6]

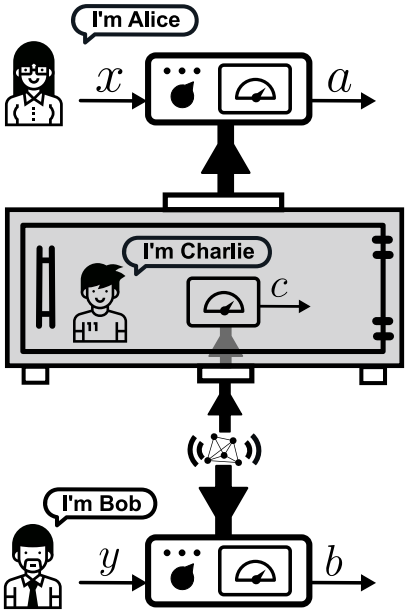

Figure 3: **Single-friend Extended Wigner's Friend Scenario.** Alice's friend Charlie, locked in an isolated lab, measures half of an entangled pair; Alice may either "PEEK" at Charlie's recorded outcome or undo his measurement and re-measure in a rotated basis, while Bob directly measures the second half of the pair.

AOE:	$\phi(ab\|xy) = \sum_c P(abc\|xy)$ for all a, b, x, y $P(a\|c, x = 1, y) = \delta_{a,c}$ for all a, c, y
LA:	$P(c\|xy) = P(c)$ for all c, x, y $P(a\|cxy) = P(a\|cx)$ for all a, c, x, y $P(b\|cxy) = P(b\|cy)$ for all b, c, x, y

These are the same requirements on P as in [3], but without Bob's friend Debbie. Following the same derivation there, the LF correlations where only Alice has a laboratory with a friend, are characterized by

$$\phi(ab|xy) = \begin{cases} \sum_c \delta_{a,c} P(b|cy)P(c) & \text{if } x = 1 \\ \sum_c P_{\text{NS}}(ab|cxy)P(c) & \text{if } x \neq 1 \end{cases}. \tag{5}$$

Using these correlations, we can give a proof of the semi-Brukner inequality. The detailed proof can be found in Appendix A. In our experiments, we still have a register for Debbie, but we restrict that to only having size one. All statements in this section still hold in that case too.

3 Experimental Program for Local Friendliness Violations with Significant Friend-Observers

The inequality violations described in Section 2 are only significant if the friends in the EWFS count as observers. In a sense, their status as observers makes the measurement outcome they observe real. While [3] showed violations with a single photonic qubit as each friend, one may reasonably doubt that photonic qubits are observers and, therefore, doubt that the experiment is significant. While running these experiments with a human as the observing friend would produce the least controversial outcome, we don't know how to do this with current technology. Instead, one can design an experimental program to build up to this scale (Figure 4).

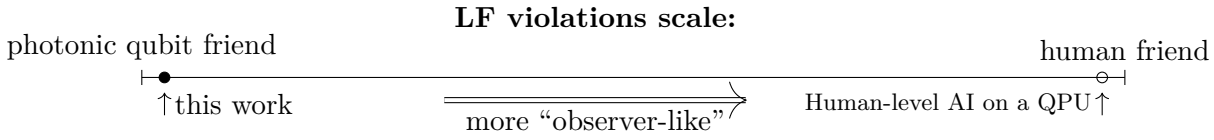

Figure 4: A program designed to test Local Friendliness violations on a progressively larger scale increases the significance of the observers used as friends. Our work gives the first experimental violations of Local Friendliness with friends larger than a photonic qubit. In [30], the authors estimate the size of a QPU needed to perform experiments using a human-level artificial intelligence simulated on a QPU as the friend observer at approximately 10^{19} logical qubits and logical depth of 10^{14} operations. We mark this as a white dot as it is a theoretical target while our work gives experimental results (black dot).

3.1 Quantifying Observerness

To establish an experimental program for more "observer-like" friends one needs to choose a physical property of a friend that "gets closer in scale to a system that is unambiguously an observer." Since there is no clear consensus on a single dimension that defines an observer, there are several dimensions that could be considered:

- More mass [31, 32].
- More complexity [33, 34].
- More objectivity [35] (e.g. redundancy and consensus via Quantum Darwinism [36]).
- Higher degree of irreversibility [37, 38, 39].
- More conscious [4, 40, 41, 42, 43, 44].
- More agency [45, 46].
- More life, according to a definition like the assembly index [47].
- More thoughtful (using a quantum computer that runs a reversible simulation of a human mind) [30].
- **Higher branch factor [48] (the focus of this work: Section 3.2).**

Fundamentally, these dimensions emerge because today there is only one kind of intuitively unambiguous observer: a human that is heavy, complex, is objectively described, whose operation appears highly irreversible, is conscious, is alive, has thoughts, and possesses agency. Observers are special and not equivalent to other quantum systems [49]. In short, different perceptual states are always macroscopically distinguishable and likely to have a high branch factor. This means that to violate LF, one needs to scale EWFSs to include observers beyond toy systems. Still, it would be surprising if one must get to an actual human to possess an observer. As John Bell inquired, "Was the wave function waiting to jump for thousands of millions of years until a single-celled living creature appeared? Or did it have to wait a little longer for some highly qualified measurer—with a PhD?" [50].

Of the options, this work focuses on the branch factor as it is a quantifiable measure that can be applied to different systems that can be prepared readily on available quantum computers. We also note previous work [35] that used quantum computers to simulate the emergence of objectivity as indicative of another direction that is compatible with quantum computers as an experimental platform.

Mass is also a compelling example of the other proposed dimensions, with several research groups working on establishing progressively larger superpositions. These are worth investigating but will require custom experimental setups, e.g., the proposed Macroscopic Quantum

Resonators MAQRO experiments that aim to test gravitational decoherence [51]. While the branch factor has the advantage that it can be run on today's quantum computers, using a universal quantum computer is overkill, as one needs only to run one program: unitary measurement and its reverse. In the future, specifically designed EWFS setups can likely be designed to maximize the branch factor.

3.2 Branch factor as a measure of observerness

In the EWFS, a quantum system in (up to normalization) a superposition of states $|\psi\rangle_0 + |\psi\rangle_1$ interacts with a friend in state $|F\rangle_{init}$ resulting in the combined state $|\psi\rangle_0 |F\rangle_0 + |\psi\rangle_1 |F\rangle_1$. The pointer states $|F\rangle_0$ and $|F\rangle_1$ are the states of the friend after having measured the system state. For our experimental program, we need a measure on these pointer states that describes how well they are acting as classical observer states. We propose using the *branch factor*, as described in [48], to quantify this "observerness".

We argue that branch factor is a natural information-theoretic metric to quantify observerness. As we review in the definitions below, a high branch factor means that operationally determining whether the friend is in a superposition of the two states or in a classical mixture of the two states would have high complexity. The hardness of distinguishing the superposition from a classical mixture should be sufficient for labeling a system as classical.

The idea is that pointer states (also called branch states) are classical when they (i) are easy to distinguish by measurements, and (ii) are hard to interfere. Interfering the branch states would operationally distinguish between there having been a classical mixture of states instead of an underlying superposition. Thus, we want interference to have high complexity. As described in [48], these conditions are sufficient to "allow the full state to be replaced with a probability distribution over the branches (a mixed state) for the purposes of natural time evolution and local measurements, so that results can be calculated separately for each branch and added probabilistically.

To mathematically define the branch factor, we first consider two complexity metrics on interference and distinguishability as defined in [52]. Let $C(U)$ be the circuit complexity of some unitary, i.e., the minimum number of one- and two-qubit unitaries required to perform U. Here, single-qubit unitaries have weight one and two-qubit unitaries have weight two. Let $|\psi_0\rangle$ and $|\psi_1\rangle$ be two orthogonal quantum states.

Definition 3.1 (Interference complexity proxy)**.** *Let* $0 \leq \delta \leq 1$*. The interference complexity* $C_I(|\psi_0\rangle, |\psi_1\rangle, \delta)$ *is equal to* $\min_U(C(U))$ *such that*

$$\frac{\| \langle\psi_1| U |\psi_0\rangle + \langle\psi_0| U |\psi_1\rangle |}{2} \geq \delta. \tag{6}$$

Definition 3.2 (Distinguishability complexity proxy)**.** *Let* $0 \leq \delta \leq 1$*. The distinguishability complexity* $C_D(|\psi_0\rangle, |\psi_1\rangle, \delta)$ *is equal to* $\min_U(C(U))$ *such that*

$$\frac{\| \langle\psi_0| U |\psi_0\rangle - \langle\psi_1| U |\psi_1\rangle |}{2} \geq \delta. \tag{7}$$

It was shown in [52] that these proxy metrics are within a constant factor $\mathcal{O}(1)$ of the true interference and distinguishability complexities [4].

Definition 3.3 (Branch factor)**.** *Let* $0 \leq \delta \leq 1$*. The branch factor* [5] *between states* $|\psi_0\rangle$ *and* $|\psi_1\rangle$ *is defined as*

$$B(|\psi_0\rangle, |\psi_1\rangle, \delta) := C_I(|\psi_0\rangle, |\psi_1\rangle, \delta) - C_D(|\psi_0\rangle, |\psi_1\rangle, \delta). \tag{8}$$

[4] Throughout this paper, we use the somewhat more abbreviated naming convention of "distinguishability complexity proxy" and "interference complexity proxy" to refer to the concepts of "distinguishability proxy" and "interference proxy", respectively.

[5] This is called "branchiness" in [48].

We consider a branch factor "good" when the interference proxy is significantly greater than the distinguishability proxy, i.e. $C_I(|\psi_0\rangle, |\psi_1\rangle, \delta) \gg C_D(|\psi_0\rangle, |\psi_1\rangle, \delta)$ for some choice of $|\psi_0\rangle$, $|\psi_1\rangle$, and δ.

To illustrate the idea behind these definitions, consider the decomposition $|\psi\rangle = \frac{|a\rangle+|b\rangle}{\sqrt{2}}$ into two branches $|a\rangle$ and $|b\rangle$. A calculation shows that observing different measurement outcome probabilities for the pure state density matrix $|\psi\rangle\langle\psi|$ and the classical mixture $\frac{|a\rangle\langle a|+|b\rangle\langle b|}{2}$ is as hard as swapping $|a\rangle$ and $|b\rangle$ [52]. This hardness is given by the interference complexity and is a measure of how many gates you need to obtain relative phase information. For good branch decompositions, we want this interference complexity to be high (so the state behaves like a classical mixture as far as the measurement outcomes are concerned), but this is not enough. It should also be relatively easy to tell the difference between the two different branches. The complexity required for this is given by the distinguishability complexity.

Some examples of states with good branch factors, as discussed in [48], are

- GHZ state: Let $n \geq 1$ be a positive integer and let $|\psi_0\rangle = |0^n\rangle$ and $|\psi_1\rangle = |1^n\rangle$. Then, for $\delta = 1$, we can exactly compute the interference and distinguishability proxy. For interference, we can use two-qubit gates $X \otimes X$ to flip the bits two at a time to swap $|0^n\rangle$ with $|1^n\rangle$. If n is even, we need $n/2$ two-qubit gates, while in the case that n is odd, we need $(n-1)/2$ two-qubit gates and one single-qubit gate. So, the interference proxy is n regardless of the parity of n. For the distinguishability proxy, we need a circuit that maps $|0^n\rangle$ to itself, but $|1^n\rangle$ to $-|1^n\rangle$. We can do this by applying one Z-gate on the first qubit. So
$$C_I = n, \quad C_D = 1, \quad \text{and} \quad B = n - 1. \tag{9}$$
- Product state and Haar random state: for n-qubit states, let $|\psi_0\rangle = |0^n\rangle$ and $|\psi_1\rangle = |\upsilon\rangle$, where $|\upsilon\rangle$ is a Haar random state. Then for $\delta = 1$ [53]
$$C_I \geq 4^n/9 - n/3 - 1/9, \quad C_D \leq n, \quad \text{and} \quad B \geq 4^n/9 - 4n/3 - 1/9, \tag{10}$$
with high probability (probability of measuring 0^n in a Haar random quantum state is $O(\exp(-n))$).
- Two random states n-qubit states produced by circuits with depth D_0 and D_1 respectively. It can be shown [48] that
$$C_I = \mathcal{O}((D_0 + D_1)n) \quad \text{and} \quad C_D = \mathcal{O}(\min(D_0, D_1)n) \tag{11}$$
- Product state and Dicke state: for n-qubit states, let $|\psi_0\rangle = |0^n\rangle$ and $|\psi_1\rangle = D(n, n/2)$ where $D(n,k)$ is a Dicke state: an equal superposition over all bitstrings of size n that have Hamming weight k. Then, for $\delta = 1$, assuming the asymptotic upper bound of the circuit complexity in [54] is also a lower bound
$$C_I \geq \Omega(n^2), \quad C_D = O(1), \quad \text{and} \quad B = \Omega(n^2), \tag{12}$$
where $B = \Omega(n^2)$ is shorthand for the statement that there is a $C > 0$ such that for all $n \geq n_0$ we have $B \geq Cn^2$ for some integer n_0. The distinguishability proxy is $O(1)$ with high probability: measuring a random qubit gives us a 1 with probability $\sim 1/2$, so measuring a constant number of qubits, one can get a success probability as high as one wants.

Examples of "bad" branch factors are those that have the reverse relationship, where the distinguishability proxy is significantly greater than the interference proxy, i.e., $C_D(|\psi_0\rangle, |\psi_1\rangle, \delta) \gg C_I(|\psi_0\rangle, |\psi_1\rangle, \delta)$ for some choice of $|\psi_0\rangle$, $|\psi_1\rangle$, and δ. As considered in [48], error-correcting codes

have bad branch factors. Making it hard for the environment to get information from your quantum system (i.e., high distinguishability) makes it less likely for your system to decohere.

In principle, one could compute the branch factor for any quantum system in a superposition of (preferred) pointer states. This includes large quantum systems like molecules, but in practice, it can be very challenging to compute the branch factor exactly.

Section 4 describes experiments where GHZ states are used to increase branch size. GHZ state friends also increase the friend's particle number and the size of the Hilbert space, which are other interesting candidates for observerness. Connecting the branch factor metric of observerness to other proposals (Section 3.1) is an open avenue for future work.

By running the EWFS with friends with progressively larger branch factors, we test LF violations for increasingly meaningful classes of observers. What could the outcomes of such a program be?

1. We could observe violations up to systems with the same branch factors as humans or even with humans as friends. Each result at each scale would provide more evidence that LF is indeed violated by reality.

2. We could observe some threshold branch factor where the LF violations stop. One could interpret this as some "collapse model" where friends above that threshold count as observers. Thus, one could argue that LF is not violated by reality. Notably, this would require some extension to textbook quantum mechanics and provide experimental evidence for a specific definition of an observer.

Of course, pursuing this program involves significant engineering challenges in reliably preparing increasing branch factors. Importantly, it also requires us to consider how to handle experiments where branch factors are produced under noisy experimental conditions. We say more about handling these noisy conditions in Section 4.1 and Section 4.2.

In the rest of the paper, we only consider the value $\delta = 1$ in the definition of branch factor. The main reason for this is the fact that the complexities are easier to analyze. Using $\delta = 1$, the values for the complexities become upper bounds, this is however not necessarily true for the branch factor.

4 Experimental Local Friendliness violations on quantum computers

In this section, we empirically demonstrate LF inequality violations using Extended Wigner's Friend Scenarios for increasing branch factors of the friend system using (i) a noiseless quantum processor simulator, (ii) a simulator with noise models, (iii), and real quantum hardware devices.

The friend system we use in this section is the GHZ state. To experimentally demonstrate these violations, we use approaches to validate branch factors produced under noise and error mitigation approaches to deal with measurement noise.

While one can consider scenarios where all local friendliness inequalities are violated, a violation of any one of inequalities is sufficient to illustrate that local friendliness has been violated. We, therefore, focus on violating the semi-Brukner inequality from Equation (1) in the following sections. The reason for focusing on this inequality is its relative simplicity. Specifically, notice that Equation (1) lacks a B_1 observable, eliminating the need to consider a PEEK setting for Bob. This simplification allows us to simplify Bob's friend (Debbie) to just a single qubit, as removing PEEK eliminates the need for Bob to look at Debbie's qubit register.[6] Removing this setting configuration from our circuit allows us to reduce the size of our circuit by approximately a factor of two. This enables us to scale the circuit and consider larger friend sizes on simulators and hardware devices that would have otherwise been more difficult to obtain. As shown in Section 2.3, the semi-Brukner inequality still holds in this case.

[6] We thank Eric Cavalcanti, Howard Wiseman, and Nora Tischler for pointing this out to us.

To compute the expectation values for the semi-Brukner inequality, we have to infer what branch the friends are in using a single measurement. Since the friend system has low distinguishability proxy for the systems we consider, this is possible with high probability. The following subsections describe how we do this for the GHZ and controlled-random unitary friend systems and plot the empirically obtained LF inequality violations.

The general form of the EWFS circuit is shown in Figure 5. Alice and Bob's measurement settings (e.g., PEEK, REVERSE-1, or REVERSE-2 as defined in Section 2.2) cause the controlled operations to be labeled as ALICE SETTING and BOB SETTING. The specific gates in these controlled operations depend on what type of friend is instantiated. Using a CNOT ladder, as in Figure 6, causes the friend system to be in a GHZ state for which we know the branch factor increases linearly in the friend's size, c.f. Equation (9). If we use a controlled-random unitary, the branch factor will increase exponentially in the friend system size, c.f. Equation (10). However, we need several gates that grow exponentially in system size to implement such a random unitary.

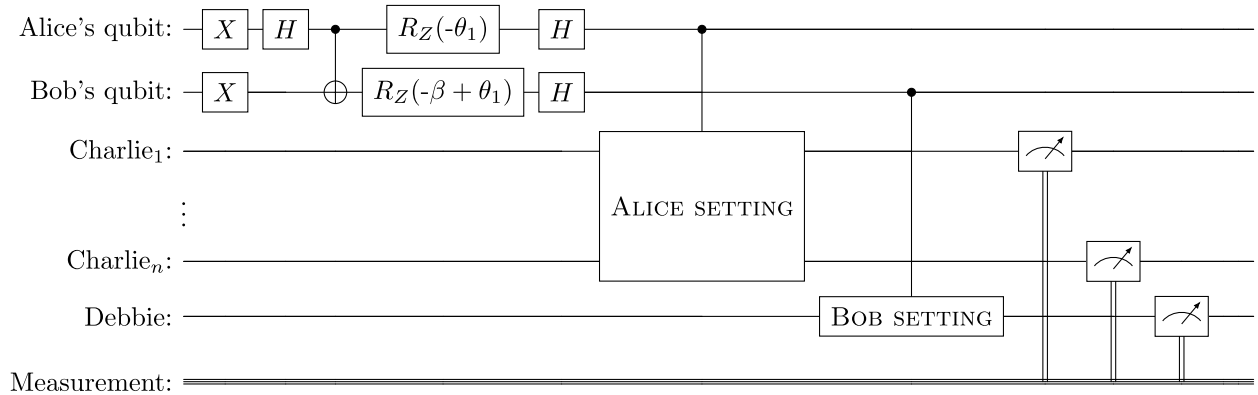

Figure 5: **Circuit depiction of the PEEK-PEEK setting for the extended Wigner's Friend scenario.** Alice and Bob begin by preparing a bipartite state as defined in Equation (2). Alice then performs her measurement setting on Charlie's qubit(s); likewise, Bob performs his measurement on Debbie's (single) qubit. The settings performed by Alice and Bob is either PEEK, REVERSE-1, or REVERSE-2. In this particular depiction of the circuit, we assume that Alice and Bob are performing the PEEK setting. Finally, the system qubits of Charlie and Debbie are measured.

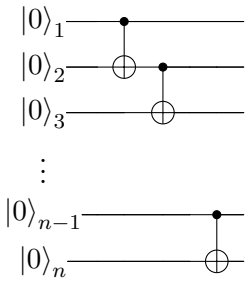

Figure 6: **CNOT ladder for GHZ friends in EWFS.** An n-qubit CNOT ladder used by Charlie in the ALICE SETTING circuit of Figure 5.

Using the circuit description of the EWFS scenario, one can quickly compute that $\langle A_i \rangle = \langle B_i \rangle = 0$ for all $i = 1, 2, 3$ and that $\langle A_i B_j \rangle = -\cos(\beta_j - \theta_i)$. This allows us to find the optimal angles for maximal violation of the semi-Brukner inequality

$$\cos(\beta_2 - \theta_1) - \cos(\beta_3 - \theta_1) + \cos(\beta_2 - \theta_3) + \cos(\beta_3 - \theta_3) - 2 \leq 0. \tag{13}$$

We give the maximum inequality violations under optimal choices of angles in the right column of Table 1.

4.1 Noisy Friends: preparing branch factors under noise

In this work, our EWFS are prepared on quantum computers, which have errors in their operation. Even if one is not using a quantum computer, any experimental setup will have noise in the prepared friend states. Thus, we need a model for dealing with LF violations where we could have errors in the branch factors of the prepared friend states.

One approach is to characterize a fidelity bound on the state of Charlie in the middle of the scenario. For example, say we aim for Charlie to be in the friend state $|\psi\rangle := \frac{1}{\sqrt{2}}|\psi_0\rangle + |\psi_1\rangle$ after they have measured their system. Errors in that preparation mean that Charlie is instead in a state represented by the density matrix ρ. Then the fidelity $\mathcal{F}(|\psi\rangle, \rho) = \langle\psi|\rho|\psi\rangle$ gives a lower bound q on the probability that the state $|\psi\rangle$ has been prepared with our target branch factor.

Our experiments must show that we have prepared the intended branch factor and violated local friendliness with those same states. We need to avoid a scenario where the incorrect states dominate the expectation values and contribute to the local friendliness violation. Consider a proposed experimental violation of the semi-Brukner inequality.

$$X := -\langle A_1 B_2\rangle + \langle A_1 B_3\rangle - \langle A_3 B_2\rangle - \langle A_3 B_3\rangle \geq 2 \tag{14}$$

When $X \geq 2$, we have an LF violation. To bound the value of X as a function of the probability q that the data going into the expectation is valid, we need to consider the worst-case scenario for the expectation values given the bounds and the probability $1-q$ of invalid data. Each random variable A_i and B_j is bounded between -1 and 1. If there is a probability q that the data is invalid, the invalid data might skew the expectation values. For invalid data, we assume the worst-case scenario where the invalid data maximizes or minimizes each term in X. The effective expectation value can be modeled as a mixture

$$\langle A_i B_j\rangle = q\langle A_i B_j\rangle^{\text{valid}} + (1-q)\langle A_i B_j\rangle^{\text{invalid}} \tag{15}$$

Similarly, for the other expectation values. Let $\langle\widetilde{A_i B_j}\rangle$ be the measured expectation value. This means that

$$\langle A_i B_j\rangle^{\text{valid}} = \frac{\langle\widetilde{A_i B_j}\rangle - (1-q)\langle A_i B_j\rangle^{\text{invalid}}}{q} \tag{16}$$

We then set $\langle A_i B_j\rangle^{\text{invalid}}$ to whatever is the worst case for that term in X. For the positive term $\langle A_1 B_3\rangle$ we have

$$\langle A_1 B_3\rangle^{\text{valid}} \geq \frac{\langle\widetilde{A_1 B_3}\rangle - 2(1-q)}{q} \tag{17}$$

For the negative terms, we have

$$-\langle A_i B_j\rangle^{\text{valid}} \geq \frac{2(q-1) - \langle\widetilde{A_i B_j}\rangle}{q} \tag{18}$$

and similarly for the other terms. This gives

$$\begin{aligned} X^{\text{valid}} &:= -\langle A_1 B_2\rangle^{\text{valid}} + \langle A_1 B_3\rangle^{\text{valid}} - \langle A_3 B_2\rangle^{\text{valid}} - \langle A_3 B_3\rangle^{\text{valid}} \\ X^{\text{valid}} &\geq \frac{1}{q}\left[\tilde{X} + 8(q-1)\right] \end{aligned} \tag{19}$$

The value of X^{valid} is what matters to show the violation under noise. We must have $X^{\text{valid}} \geq 2$ or similarly, the measured value

$$\tilde{X} \geq 8 - 6q. \tag{20}$$

The maximum value for $\tilde{X}$ in the Semi-Brukner inequality is 2.82843 (See Table 1). Solving for the minimum fidelity that supports this gives 93.66%. Thus, we don't need perfect friend state preparation to see violations. If our friend state is prepared with greater than 93.66%, then we can be confident that our LF violations hold at our target branch factor.

Now, we consider how to characterize q from a real experiment. One approach is to do state tomography and measure it directly. Unfortunately, this becomes experimentally difficult for larger friend sizes. Instead, we propose extrapolating from a depolarizing model for the quantum circuit.

Depolarizing Case: Assume a depolarizing noise model where we apply the depolarizing channel after each single-qubit gate in the circuit with parameter p_1 and with parameter p_2 after each two-qubit gate, i.e., $\mathcal{E}(\rho) = (1-p_i)\rho + p_i I/2^n$ for n-qubit quantum state ρ. Then it is straightforward to check that if our circuit with n single-qubit gates and m two-qubit gates are supposed to prepare the quantum state $\rho = |\psi\rangle\langle\psi|$, the noisy density matrix will be $\rho' = (1-p_1)^n(1-p_2)^m\rho + (1-(1-p_1)^n(1-p_2)^m)I/2^n$. Since the above observables are zero when evaluated at the maximally mixed state, then by linearity of the expectation value, the expected values of the observables for the noisy density matrix ρ' will be equal to the ideal one multiplied by $(1-p_1)^n(1-p_2)^m$. Thus, we'd need $\tilde{X} \geq 2/[(1-p_1)^n(1-p_2)^m]$ to show a violation. Again, using the max value of 2.82843 for $\tilde{X}$, we see that the minimum single-qubit and two-qubit fidelities should satisfy $(1-p_1)^n(1-p_2)^m \geq 2/2.82843 \approx 0.707$. Usually, the two-qubit gate fidelity $1-p_2$ is much lower than the single-qubit gate fidelity, and the preparation of the friend size mostly dominates the number of two-qubit gates. Linearly increasing friend size increases the two-qubit gates linearly, assuming a chain-like layout for the friend system.

For a circuit with 10 layers of gates (where each layer represents one step of parallel gate operations in the circuit depth), assuming $p_1 = p_2/10$ and $n = 10m$ (single-qubit gates being an order of magnitude higher fidelity and friend system preparation requiring an order of magnitude more single-qubit gates), this would need a two-qubit gate error rate of at most $\sim 1.7\%$. This is not an infeasible error rate for near-term quantum computers, but to scale to a circuit with 100 layers of depth, that error rate also drops by an order of magnitude. If depolarizing noise is a good error model; each order of magnitude decrease in error-rate should allow one to push to another order of magnitude in friend size and branch factor. Fault-tolerant quantum computers will be critical here.

4.1.1 Other approaches to validate branch factors

The approach described above bootstraps up to estimated fidelities from characterizing modular components. One might prefer a systematic witness for branch factor that doesn't require such extrapolation.

Consider the case where friend states are given by two Haar random states whose interference and distinguishability proxies are then given by (11). We know there is a signature for random quantum states given by heavy output distributions whose statistics can act as a proxy for having prepared random quantum states [55]. This would give a protocol for validated EWFS experiments where one randomly interleaves the true experiment, gathering Alice and Bob's statistics, or validations where computational basis measurement statistics are taken on Charlie's and/or Debbie's qubits. The measurements from the validation runs can be verified using cross-entropy benchmarking following [55].

A downside of this direction is that this verification is computationally intensive, requiring classical simulation of the circuits to do the cross-entropy benchmarking. Thus, this approach is likely limited to $\leq$ 100 qubits. Instead, a validation-based collision counting of random quantum states would not require much classical computing but does require a large amount of sampling [56]. Another alternative is to consider "peaked" random circuits proposed for efficient validation [57]. However, more work needs to be done to study the preparation and branch

factors of superpositions of these states.[7]

More broadly, we would prefer classically efficient verifications that the quantum states of sufficient branch factor have been produced. In [58], the authors introduce a protocol for classically verifying a quantum system's dynamics using CHSH tests. More examples of "self-testing" to verify the production of specific quantum states are given in this survey [59]. For example, in [60] a protocol is given to use single-mode Gaussian measurements to verify a class of continuous variable quantum states, including Boson Sampling states. This class of states could be used to design friends who have high branch factors but also efficient state verification. We leave it to future work to directly link the self-testing literature to validating branch factors, but note that this direction looks promising for scaling up validations.

4.2 Noisy Measurements: inferring observed outcomes using majority vote

After measurement, there are many ways to infer the friend's outcome in the PEEK setting. A simple way would be to randomly pick a qubit from the friend system and measure it. In the noiseless case, this would work perfectly to determine the outcome of the GHZ state. An example circuit of EWFS using this approach is in Figure 7. However, this will not work well in the presence of measurement noise since bits might get flipped by measurement errors. A better approach would be to measure multiple qubits and decide which outcome you have measured based on a majority vote. Figure 8 shows an example where we measure all the qubits of the friend system in the PEEK setting. The observables we are interested in assign a value of 1 to one outcome and a value of -1 to the other.

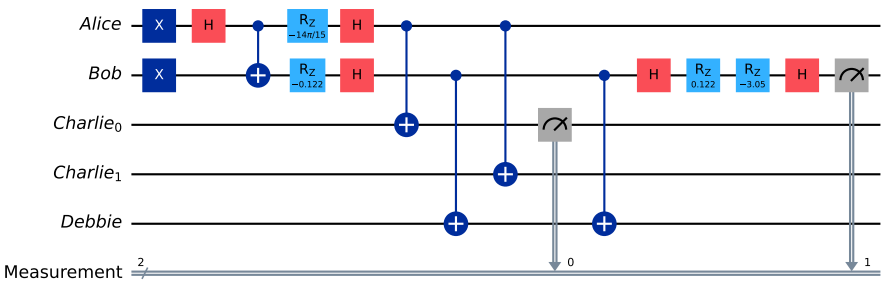

Figure 7: **Example EWFS circuit with PEEK and REVERSE-1 settings.** An example of the EWFS circuit with GHZ friends using the random strategy, where the friend Charlie consists of two qubits. Alice uses a PEEK setting in this example circuit, while Bob uses the REVERSE-1 setting.

For the case of GHZ friends, when measuring the all-zero state in the computational basis, we want to assign a value of 1, and when measuring the all-ones state, we assign a value of -1. In the presence of noise, other bitstrings can be measured as well. We use the majority vote to determine the value of the other bitstrings. If n is the size of the friend system, which we assume to be odd, the measurement consists of the following positive semidefinite matrices

$$F_0 = \sum_{H(x)<n/2} |x\rangle\langle x| \quad \text{and} \quad F_1 = \sum_{H(x)>n/2} |x\rangle\langle x| \tag{21}$$

where $H(x)$ is the Hamming weight of the n-bit string x. The observable for Alice is then simply

$$A = F_0 - F_1. \tag{22}$$

[7] We thank Andrea Mari for pointing out these recent works on validation to us.

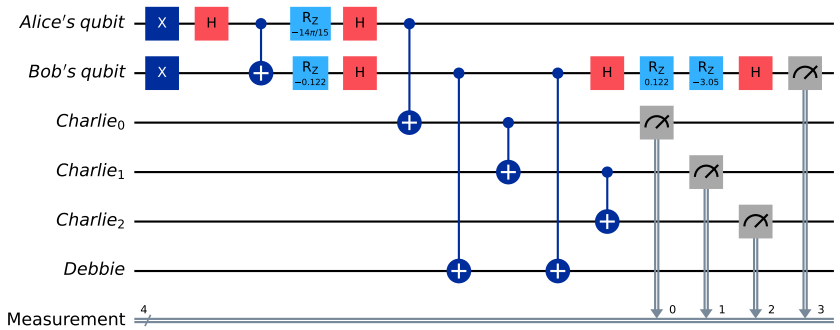

Figure 8: **EWFS circuit where Alice measures all qubits of Charlie.** An example of the EWFS circuit with GHZ friends using the majority vote strategy, where the friend Charlie consists of three qubits. Alice uses a PEEK setting in this example circuit, while Bob uses the REVERSE-1 setting. Note that Alice is measuring all the qubits of her friend in this case.

The observable B for Bob is defined similarly.

In the ideal scenario, when there is no noise, the violations of the LF inequalities should match the approach where we infer the friend's observed outcome by measuring a random qubit of the friend. However, as we introduce noise, while the magnitude of the LF violations will be the same on average, there will be more variation in the random approach. We demonstrate this by comparing the simulated violations using these two approaches. The results of running the EWFS, where we measure just one qubit of the friend system vs. the use of the majority vote observable for GHZ friends of increasing qubit sizes on quantum simulators using depolarizing noise and readout error are depicted in Figure 9.

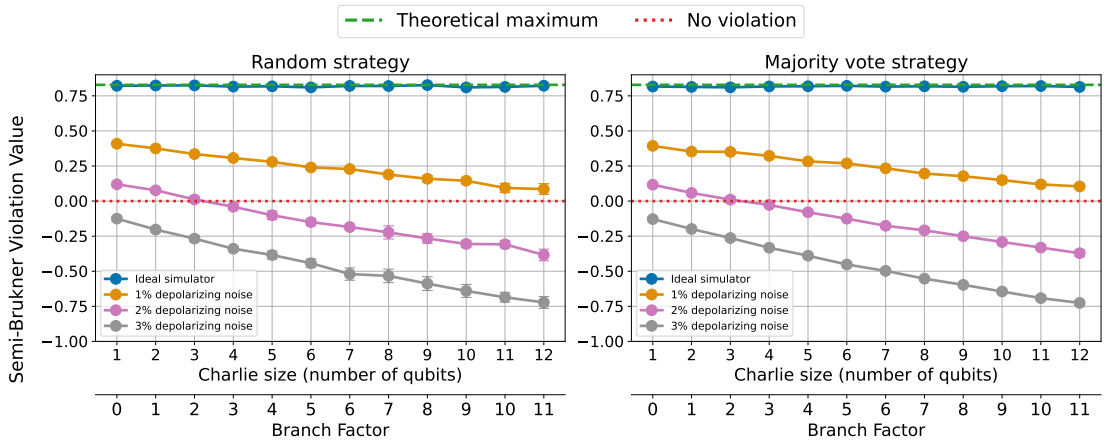

Figure 9: **A comparison between the "random" and "majority vote" strategies for EWFS.** Each plot considers how each strategy performs for progressively increasing depolarizing noise levels with fixed 1% readout error on all qubits. Each data point is run using 10000 shots and averaged over 10 trials. The bottom x-axis ranges over the number of qubits in the quantum system size of Charlie, while the top x-axis shows the corresponding branch factor. One can see there is minimal difference between the two approaches, except that the majority vote approach has less variance.

This majority vote approach is one form of readout error mitigation, and future work can apply more of these methods. For example, stabilizer checks on the friend's unitary operation can be used for error detection and post-selection. A bit-flip error in constructing the GHZ

state for Charlie still results in states with the same branch factor. One can consider this bit flip like a relabeling of the "logical" GHZ states from, for example, $|000\rangle = |O\rangle_L; |111\rangle = |1\rangle_L$ to $|001\rangle = |O\rangle_L; |110\rangle = |1\rangle_L$. However, Alice needs to know on which qubit the error occurred to not incorrectly infer what branch Charlie is in. In this case, tracking an error on the third qubit means Alice can assign the inverse of its measurement. As quantum processors become more sophisticated, the full suite of error mitigation and correction techniques can be deployed to characterize the target friend states with high fidelity.

4.3 Experimental Results: LF Violations using GHZ friend states on quantum computers

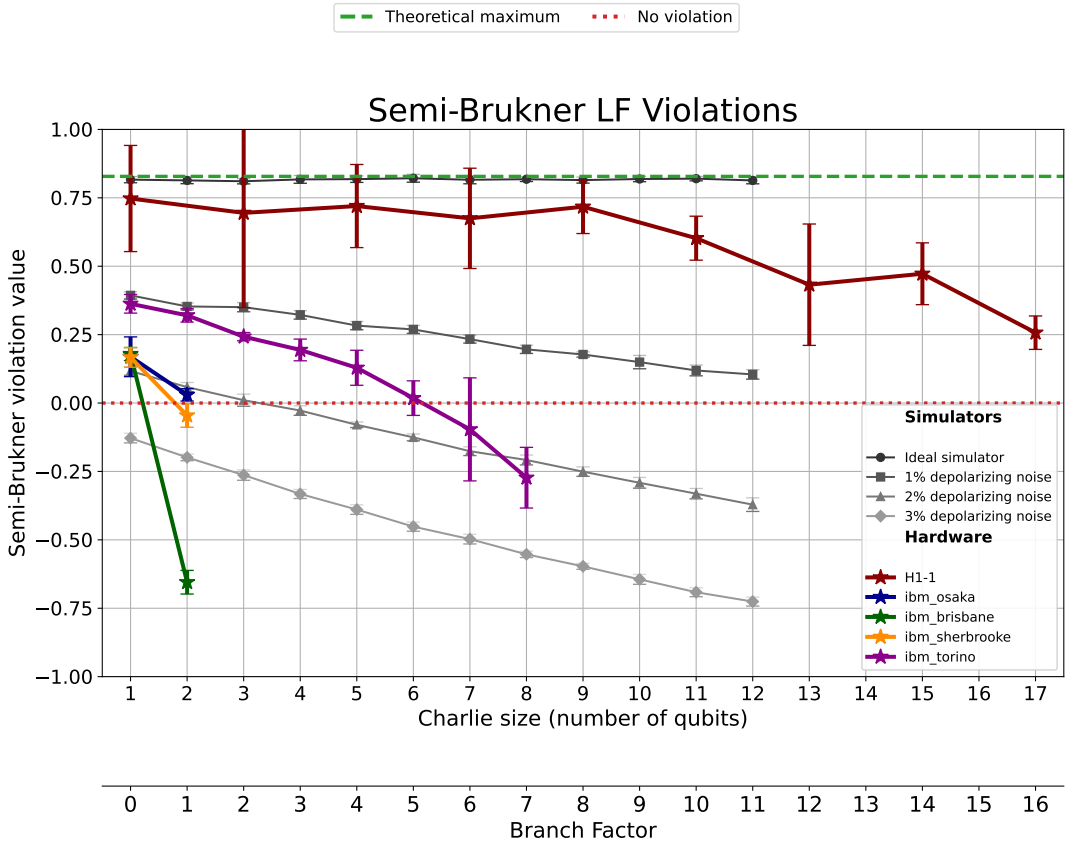

Figure 10: **A comparison between simulator, noisy emulator, and hardware for majority vote EWFS.** The gray-scaled lines show how increasing the depolarizing noise reduces the maximum friend size for which a violation occurs. The lines in color show the `ibm_osaka`, `ibm_sherbrooke`, `ibm_torino` IBM hardware devices and the H1-1 Quantinuum hardware device. Note that the only IBM hardware device to obtain violations beyond branch factor 0 is `ibm_torino`, showing a violation at branch factor 4, while on the H1-1 device, we obtain a violation at branch factor 16. We transpile the circuit before running for the specific coupling map topology for the emulated and real hardware. Further details on the transpilation are provided in Appendix B. For each line in the plot, the bottom x-axis ranges over the number of qubits in the quantum system size of Charlie, while the top x-axis shows the corresponding branch factor. All IBM data points are run with 10000 shots over 10 trials. For the H1-1 device, we ran each experiment with 200 shots and 4 trials, except for the experiment of size 17, which we ran for 7 trials. Error bars are 3 standard deviations.

Using the majority vote approach for measurement described previously, we perform experiments on IBM superconducting quantum computers to measure violations. Results from noisy model simulations and hardware experiments are plotted in Figure 10. These experiments use the majority vote implementation of EWFS from Section 4.2. In these plots, the y-axis is the value of the Semi-Brukner violation on the left-hand side of the inequality in Equation (1). Thus, we have a violation when this value is above 0, as indicated by the red dotted line. The green

dotted lines indicate the maximum achievable theoretical value of 0.82843 (see Section 4). We plot these violations for experiments where the friend is prepared in a GHZ state of increasing qubit number (bottom x-axis) corresponding to branch factors indicated on the top x-axis. The point where the violation value crosses below the dotted red line is the maximum branch factor for which we can show violations on that backend.

The leftmost plot shows results from a simulated backend running perfect simulations or quantum circuits at 1%, 2%, and 3% per gate depolarizing noise rates. Perfect simulations have no limit to the size of violations we expect to see, corresponding to the predictions of textbook quantum mechanics. For each noise rate, we see violations decrease such that a 2% per gate noise rate would only support violations to branch factor 9, and a 3% per gate noise rate supports a validation up to branch factor 4. These depolarizing simulations do not include any specific gate set or qubit topology compilations. Thus, we expect them to be optimistic predictions for real experiments where that compilation adds additional overhead.

The middle plot shows violations on various hardware emulators, including more sophisticated noise models based on several superconducting and one ion trap emulator.

The rightmost plot shows violations obtained directly on quantum hardware: IBM's superconducting quantum processors Osaka, `ibm_sherbrooke`, and `ibm_torino`. While `ibm_osaka` and `ibm_sherbrooke` do not show violations beyond branch factor 0, the `ibm_torino` processor supports violations up to branch factor 4. Importantly, fidelity is not the only driver of performance here. The `ibm_torino` processor's native gates are better suited to our circuit, so it also has much lower gate counts, improving performance. On the H1-1 Quantinuum device [61], we obtained a violation at the branch factor of as high as 16.

4.3.1 Validation of branch factor preparation

We use the methods in Section 4.1 to validate our violations on real hardware. This section shows that we need confidence that our friend state is prepared with a state fidelity of greater than 93.66% to ensure LF violations have been shown in the worst case. To estimate the friend's state fidelity, we count the gates needed to prepare the state and use the per-gate single and two-qubit error fidelities for the devices. IBM Torino has a single and two-qubit gate errors that are sufficiently low to show violations up to branch factor 9, while for the Quantinuum H1-1 device the errors are low enough to allow for much higher branch factor violations, higher than branch factor 16 that we observed violations for. In Figure 11, we plot the estimated friend state fidelity vs. branch factor and the single and two-qubit gate counts for various hardware backends.

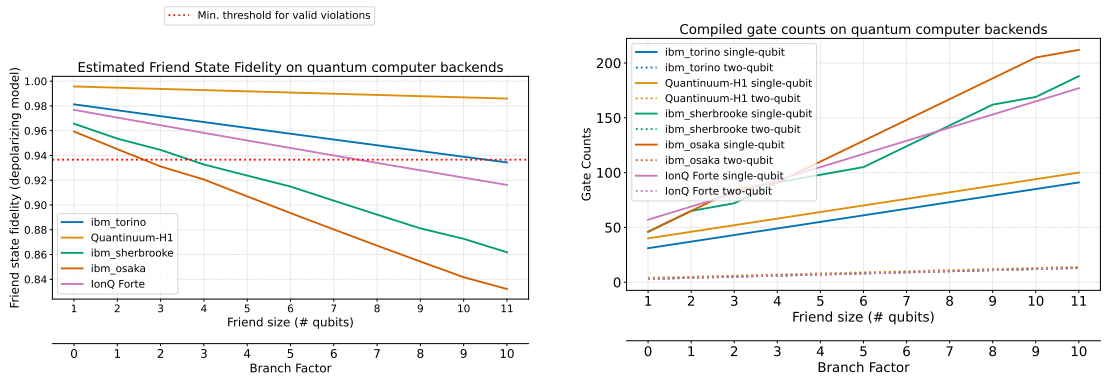

Figure 11: (Left) A plot of the estimated fidelities of the friend state when prepared on different backends using the depolarizing model to estimate fidelity. The IBM Torino device supports valid LF violations up to branch factor 7, while the H1 device could theoretically support much larger violations. (Right) The single and two-qubit gate counts for compiled EWFS circuits on different backends.

5 More branch factor from less QPU: controlled-random unitary friends and Dicke states

In Section 4.3, we showed violations using only GHZ friends. However, it is reasonable to consider whether other friend states might produce higher branch factors with the same limited noisy experimental resources. This section discusses approaches and available resource tradeoffs when preparing different friend states while targeting higher branch factors. We find that if you can use longer quantum circuits for the friend states, you achieve higher branch factor with the same number of qubits using Dicke states or controlled-random unitary states instead of GHZ states.

We may want to use quantum states for the friend system, where the branch factor grows quickly as we increase the number of qubits. In the case of the GHZ friends, we saw in Equation (9) that the branch factor increases linearly in the number of qubits. However, when we use a controlled-random unitary, the branch factor increases exponentially in the number of qubits, c.f. Equation (10). Controlled-random unitary friends will obtain higher branch factors for the same number of qubits. Implementing a controlled-random unitary friend can be done by picking a Haar random unitary matrix and compiling it to a controlled quantum circuit.

Inferring the branch of a controlled-random unitary friend is similar to the GHZ case. We have two branches, the zero-state $|0^n\rangle$ and a Haar-random state $|\psi\rangle$. In the noiseless case, we can distinguish with increasingly high probability the two branches with just one measurement: if you measure a non-zero bitstring, the branch is $|\psi\rangle$. If you measure $|0^n\rangle$, the branch could have been $|\psi\rangle$, but the probability of this goes to zero exponentially fast as n grows. This is more challenging in the presence of noise, mainly because the branch $|0^n\rangle$ might evolve to a superposition of non-zero bitstrings. However, the highest amplitude should still be on the $|0^n\rangle$ state, so with high probability, we will still correctly infer the correct branch. The relevant observable in this case is, therefore, given by

$$A = |0^n\rangle\langle 0^n| - \sum_{x \neq 0^n} |x\rangle\langle x|. \tag{23}$$

We observe violations by running the EWFS circuits in an ideal simulator using the controlled-random unitary friends, which is observable for inferring branches. With small depolarizing noise, we still obtain violations for a few qubits; see Figure 13. However, it looks to be challenging to show these same violations on today's quantum hardware. The main reason is that the Haar random unitaries are very complex because they require many single and two-qubit gates from some fixed gate-set required from the hardware. Still, more sophisticated processors will eventually be capable of delivering this performance. [8]

One way to obtain violations using such (complicated) circuits on noisy hardware is to use states easily distinguishable from the all-zero state, even in the presence of noise, while having a high swap complexity with the all-zero state. For example, states with this property are Dicke states [54]. These are quantum states on n qubits with amplitudes only on bitstrings with a Hamming weight of k for a choice of $0 \leq k \leq n$ denoted by $D(n, k)$. In [54], they show quantum circuits with circuit complexity $O(kn)$. Assuming this is also a lower bound, the equal superposition of such a state and the all-zero state would have branch factor $\Omega(kn)$. For example, take $k = n/2$, so $D(n, n/2)$ is an equal superposition over bitstrings with Hamming weight $n/2$ and has circuit complexity $O(n^2)$. In the presence of bitflip noise, it is unlikely that too many bits get flipped to get close to the all-zero state. In this way, even in the presence of noise, we are unlikely to measure the all-zero state. Also, the noisy all-zero state will have amplitudes

[8] Note that supremacy experiments [55] are similar but not quite the same as what is needed. Here, we need not just Haar-random unitaries but also controlled Haar-random unitaries. This increases the challenge for quantum processors.

on non-zero bitstrings, but these will probably have low Hamming weight. For example, the observable

$$A = \sum_{H(x)<n/3} |x\rangle\langle x| - \sum_{H(x)\geq n/3} |x\rangle\langle x| \tag{24}$$

should be able to infer the right branch with high probability in the presence of bitflip noise. Still, these states are too complex (with many single-qubit gates and CNOTs) to run on noisy hardware and obtain violations. In Figure 13, we show some violations of the semi-Brukner inequality for small values of depolarizing noise. In Figure 12, we plot the number of gates required to implement a Haar random unitary and GHZ states on n qubits versus the branch factor. For the random unitary, we use the lower bound on the branch factor 10, whereas for the GHZ states, we use the exact value 9. We don't have a plot for Dicke states as that would require an explicit lower bound, including constant factors on the circuit complexity. However, we conjecture that it will lie between the GHZ state and the random unitary resource requirements for both gates and qubits.

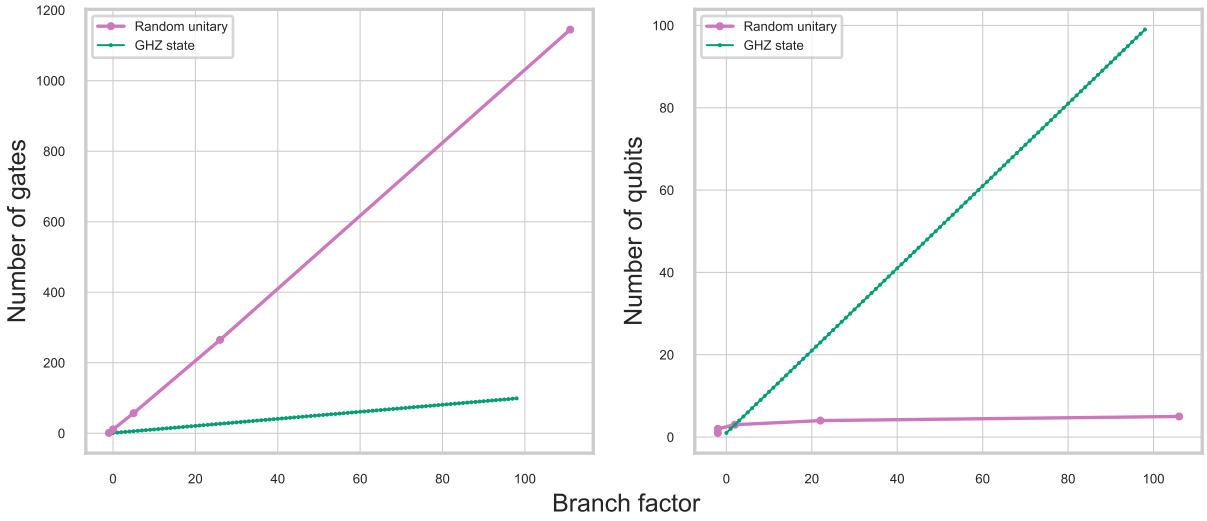

Figure 12: **Number of single and two-qubit gates and number of qubits required to prepare random unitary and GHZ states vs. branch factor.** For the basis gate set, we use the single qubit X, Y, and Z rotations and CNOT gate, and we use Qiskit to transpile the given circuits. We see a tradeoff available for increasing branch factors depending on whether one is minimizing qubit number or gate count. Focusing on lower gate counts makes GHZ friends preferable while focusing on smaller numbers of qubits makes random unitary friends more preferable.

In Section 4.1.1, we consider several types of random quantum states that may be of interest because they have protocols (of varying difficulty) to validate their preparation. Future work should consider whether these states can also efficiently generate large branch factors with limited qubit counts and gate numbers.

6 Future Directions

This work introduces a program for testing Local Friendliness using observers of increasingly significant branch factors. We explain how quantum computers of increasing power can run these Local Friendliness tests using Extended Wigner's Friend scenarios. We then show violations of Local Friendliness at small scales using currently available superconducting processors.

It is important to note that the LF violations shown in this work are not *loophole-free*. For example, we have not used the speed-of-light limitations on communication to separate Alice and Charlie from Bob and Debbie. In principle, loophole-free Local Friendliness violations could

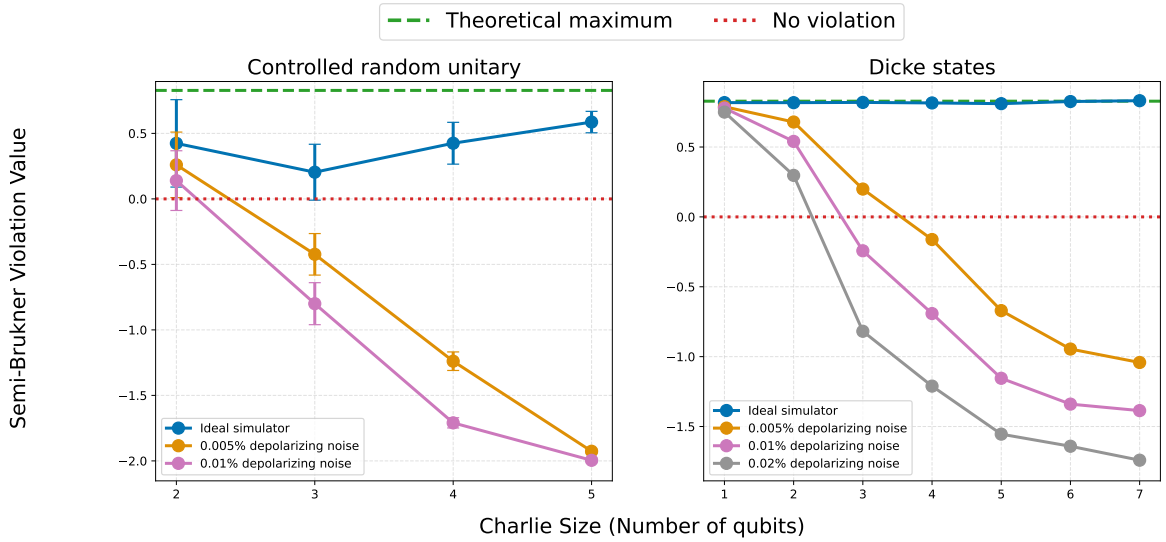

Figure 13: **Inequality violation values for the semi-Brukner inequality over an increasing range of depolarizing noise.** On the left, we consider a controlled-random unitary acting as the friends. On the right, we consider a controlled Dicke state as a friend. For the controlled-random unitary friends, we sample a Haar random unitary 100 times and take the average and error bars resulting from those runs. In the random unitary case, one sees that we don't obtain the optimal violation even in the ideal simulations. The reason is that inferring branches is probabilistic and fails with higher probability in the low friend sizes.

be performed with networked quantum computers over a quantum internet [62]. Many proposals exist for building these quantum links today, with companies and research groups investing in building them at scale. We anticipate that, as quantum computers improve, quantum networks connecting them will also improve. Further, EWFS only needs two nodes to be connected by a quantum link. Thus, Local Friendliness violations are an appealing fundamental science application for the next generations of quantum computers and early quantum networks.

While this work ran EWFS on superconducting and ion-trap quantum processors available over the cloud, other types of quantum processors, including neutral atoms, silicon, and others, are being developed. As these platforms evolve, some specific properties may be helpful for LF violations. For example, many neutral atom platforms can natively execute global CZ gates [63, 64]. Combined with the increasing number of qubits available in neutral atom platforms, neutrals could be well suited to producing the GHZ-type states we seek in larger and larger friends.

Furthermore, we could consider designing quantum processing systems optimized for producing LF violations at progressively larger branch factors. In a sense, general-purpose quantum computers are overkill for running EWFS. We do not need flexible re-programmability. Instead, we need to produce, for example, a specific controlled-random unitary (or GHZ state) that we can reverse unitarily. Perhaps a quantum ASIC or purpose-built quantum system can scale to a significant branch factor with fewer engineering difficulties than needed for a large fault-tolerant quantum computer. It may even be that EWFS, with more than two friends and more choices of measurement settings for Alice and Bob, might be advantageous in matching theory with easily buildable experiments. Designing experimental systems can optimize performance both by increasing the branch factor for fixed resources and also by preparing states whose branch factor can be easily verified, as discussed in Section 4.1.1. This is a fresh direction for scaling up controlled quantum systems for fundamental research.

Finally, there is an important outstanding theoretical question. What branch factors should we aim for? Ideally, we would have milestones of specific branch factor sizes corresponding to ruling in or out meaningful classes of physical systems as observers. For example, what is the branch factor of a single photon detector, the human eye, or the human brain? This would add

meaningful threshold milestones to experiments in the program of Figure 4.

One approach is to work backward from physical systems that arguably most resemble human observers. This is the approach taken in [30], where the authors consider a reversible simulation of a human-level artificial intelligence running on a QPU as the friend (QUALL-E). The authors estimate the size of a QPU needed to perform experiments using a human-level artificial intelligence simulated on a QPU as the friend observer at approximately 10^{19} logical qubits and logical depth of 10^{14} operations. While we don't know the details of what branch factor such a simulation might produce, we can estimate that a QPU capable of running such a simulation could also produce GHZ states with a branch factor of order 10^{19} as GHZ branch factors scale with qubit number.

Alternatively, we can take inspiration from other experiments where the quantum-classical cut is placed. In the loophole-free Bell violations [65], the experimenters needed to determine at what point it was sufficient to declare the information classical in the measurement chain. For reference, in [65] Figure 2 shows the spacetime diagram ending at the end of the detection period. After this point, sufficient separation to ensure no loopholes was no longer needed. This indicates that there is some accepted physical system that becomes classical before it reaches a human. Calculating the corresponding branch factor for this system would give a meaningful target. Future work can look to calculate these branch factors for other meaningful systems to produce a road map of increasingly meaningful Local Friendliness violations.

Code availability

Software that implements the EWFS circuit and the code used to generate the data and plots in this work are available on GitHub at [66].

Acknowledgments

We thank Eric Cavalcanti and Nora Tischler for discussing encoding the EWFS into a quantum circuit, providing the data in the middle column of Table 1. We additionally thank them, as well as Eleanor Rieffel, Veronika Baumann, and Andrea Mari, for their comments on the drafts of this manuscript. We thank Howard Wiseman, Časlav Brukner, Felix Binder, and all the Wigner's Friends workshop attendees for suggestions and discussion. VR thanks Kevin Sung, Jake Lishman, and Luciano Bello for discussions on Qiskit and running on IBM hardware. We also thank the Nexus team for guiding our experiments on the Quantiuum H1 device. VR and FL thank Matthew Beach for extensive debugging and assistance in running experiments via the Braket platform. WZ thanks the O'Shaughnessy Fellowship for support of this work. This work was supported in part by ARC Grant No. DP250102162.

References

[1] Abner Shimony. "Search for a worldview which can accommodate our knowledge of microphysics". Philosophical consequences of quantum theoryPages 25–37 (1989).

[2] Eric G Cavalcanti. "Reality, locality and all that:" experimental metaphysics" and the quantum foundations" (2008).

[3] Kok-Wei Bong, Aníbal Utreras-Alarcón, Farzad Ghafari, Yeong-Cherng Liang, Nora Tischler, Eric G Cavalcanti, Geoff J Pryde, and Howard M Wiseman. "A strong no-go theorem on the Wigner's friend paradox". Nature Physics **16**, 1199–1205 (2020).

[4] Eugene P Wigner. "Remarks on the mind-body question". In The Scientist Speculates. Pages 284–302. Heinemann (1961).

[5] Marwan Haddara and Eric G Cavalcanti. "A possibilistic no-go theorem on the Wigner's friend paradox" (2022).

[6] Howard M Wiseman. "The two Bell's theorems of John Bell". Journal of Physics A: Mathematical and Theoretical **47**, 424001 (2014).

[7] Howard M Wiseman and Eric G Cavalcanti. "Causarum investigatio and the two Bell's theorems of John Bell". Quantum [Un] Speakables II: Half a Century of Bell's TheoremPages 119–142 (2017).

[8] David Deutsch. "Quantum theory as a universal physical theory". International Journal of Theoretical Physics **24**, 1–41 (1985).

[9] Eric G Cavalcanti. "The view from a Wigner bubble". Foundations of Physics **51**, 39 (2021).

[10] Nick Ormrod and Jonathan Barrett. "Quantum influences and event relativity" (2024).

[11] Laurens Walleghem, Rui Soares Barbosa, Matthew Pusey, and Stefan Weigert. "A refined Frauchiger–Renner paradox based on strong contextuality" (2024).

[12] V Vilasini and Mischa P Woods. "A general quantum circuit framework for extended Wigner's friend scenarios: Logically and causally consistent reasoning without absolute measurement events" (2022).

[13] Eric G Cavalcanti, Andrea Di Biagio, and Carlo Rovelli. "On the consistency of relative facts". European Journal for Philosophy of Science **13**, 55 (2023).

[14] Emily Adlam and Carlo Rovelli. "Information is physical: Cross-perspective links in relational quantum mechanics" (2022).

[15] Marcin Markiewicz and Marek Żukowski. "Relational quantum mechanics with cross-perspective links postulate: an internally inconsistent scheme" (2023).

[16] Carlo Rovelli. "Relational quantum mechanics". International journal of theoretical physics **35**, 1637–1678 (1996).

[17] Stefan Teufel and Detlef Dürr. "Bohmian mechanics: The physics and mathematics of quantum theory". Springer. (2009).

[18] Časlav Brukner. "On the quantum measurement problem". Quantum [un] speakables II: half a century of Bell's theoremPages 95–117 (2017).

[19] Časlav Brukner. "A no-go theorem for observer-independent facts". Entropy **20**, 350 (2018).

[20] Daniela Frauchiger and Renato Renner. "Quantum theory cannot consistently describe the use of itself". Nature communications **9**, 3711 (2018).

[21] Nuriya Nurgalieva. "Multi-agent epistemic paradoxes in physical theories". PhD thesis. ETH Zurich. (2023).

[22] Jochen Szangolies. "The quantum Rashomon effect: A strengthened Frauchiger-Renner argument" (2020).

[23] David Schmid, Yìlè Yīng, and Matthew Leifer. "A review and analysis of six extended Wigner's friend arguments" (2023).

[24] Marwan Haddara and Eric G. Cavalcanti. "Local friendliness polytopes in multipartite scenarios" (2024).

[25] Veronika Baumann and Caslav Brukner. "Observers in superposition and the no-signaling principle" (2023).

[26] Roger Colbeck. "Quantum and relativistic protocols for secure multi-party computation" (2009).

[27] Stefano Pironio, Antonio Acín, Serge Massar, A Boyer de La Giroday, Dzmitry N Matsukevich, Peter Maunz, Steven Olmschenk, David Hayes, Le Luo, T Andrew Manning, et al. "Random numbers certified by Bell's theorem". Nature **464**, 1021–1024 (2010).

[28] Antonio Acín and Lluis Masanes. "Certified randomness in quantum physics". Nature **540**, 213–219 (2016).

[29] Erik Woodhead. "Imperfections and self testing in prepare-and-measure quantum key distribution". PhD thesis. Ph. D. thesis, Université libre de Bruxelles. (2014).

[30] Howard M Wiseman, Eric G Cavalcanti, and Eleanor G Rieffel. "A thoughtful Local Friendliness no-go theorem: a prospective experiment with new assumptions to suit". Quantum **7**, 1112 (2023).

[31] Yaakov Y Fein, Philipp Geyer, Patrick Zwick, Filip Kiałka, Sebastian Pedalino, Marcel Mayor, Stefan Gerlich, and Markus Arndt. "Quantum superposition of molecules beyond 25 kDa". Nature Physics **15**, 1242–1245 (2019).

[32] Uroš Delić, Manuel Reisenbauer, Kahan Dare, David Grass, Vladan Vuletić, Nikolai Kiesel, and Markus Aspelmeyer. "Cooling of a levitated nanoparticle to the motional quantum ground state". Science **367**, 892–895 (2020).

[33] Alexei Grinbaum. "Quantum observer and Kolmogorov complexity: A model that can be tested" (2010).

[34] Markus P Müller. "Law without law: From observer states to physics via algorithmic information theory". Quantum **4**, 301 (2020).

[35] Diana A Chisholm, Guillermo García-Pérez, Matteo AC Rossi, Sabrina Maniscalco, and G Massimo Palma. "Witnessing objectivity on a quantum computer". Quantum Science and Technology **7**, 015022 (2021).

[36] Wojciech Hubert Zurek. "Quantum Darwinism". Nature physics **5**, 181–188 (2009).

[37] Sreenath K Manikandan, Cyril Elouard, and Andrew N Jordan. "Fluctuation theorems for continuous quantum measurements and absolute irreversibility". Physical Review A **99**, 022117 (2019).

[38] Maitreyi Jayaseelan, Sreenath K Manikandan, Andrew N Jordan, and Nicholas P Bigelow. "Quantum measurement arrow of time and fluctuation relations for measuring spin of ultracold atoms". Nature communications **12**, 1–7 (2021).

[39] Emanuel Schwarzhans, Felix C Binder, Marcus Huber, and Maximilian PE Lock. "Quantum measurements and equilibration: The emergence of objective reality via entropy maximisation" (2023).

[40] Abner Shimony. "Role of the observer in quantum theory". American Journal of Physics **31**, 755–773 (1963).

[41] Henry P Stapp. "Attention, intention, and will in quantum physics". Journal of Consciousness studies **6**, 143–143 (1999).

[42] Stuart Hameroff and Roger Penrose. "Consciousness in the universe: A review of the 'orch or'theory". Physics of life reviews **11**, 39–78 (2014).

[43] Hartmut Neven, Peter Read, Kenneth S Kosik, Tjitse Van der Molen, Dirk Bouwmeester, Eve Bodnia, Luca Turin, and Christof Koch. "Testing the conjecture that quantum processes create conscious experience". Preprints (2024).

[44] Tim Bayne, Anil K Seth, Marcello Massimini, Joshua Shepherd, Axel Cleeremans, Stephen M Fleming, Rafael Malach, Jason B Mattingley, David K Menon, Adrian M Owen, et al. "Tests for consciousness in humans and beyond". Trends in cognitive sciences (2024).

[45] Vedran Dunjko, Jacob M Taylor, and Hans J Briegel. "Quantum-enhanced machine learning". Physical review letters **117**, 130501 (2016).

[46] Hartmut Neven, Peter Read, and Tobias Rees. "Do robots powered by a quantum processor have the freedom to swerve?" (2021).

[47] Abhishek Sharma, Dániel Czégel, Michael Lachmann, Christopher P Kempes, Sara I Walker, and Leroy Cronin. "Assembly theory explains and quantifies selection and evolution". Nature **622**, 321–328 (2023).

[48] Jordan K. Taylor and Ian P. McCulloch. "Wavefunction branching: When you can't tell pure states from mixed states". Quantum **9**, 1670 (2025).

[49] Časlav Brukner. "Qubits are not observers–a no-go theorem" (2021).

[50] John S Bell, C Isham, R Penrose, and D Sciama. "Quantum mechanics for cosmologists". John S Bell On The Foundations Of Quantum Mechanics **99**, 125 (2001).

[51] Rainer Kaltenbaek, Markus Arndt, Markus Aspelmeyer, Peter F Barker, Angelo Bassi, James Bateman, Alessio Belenchia, Joel Bergé, Sougato Bose, Claus Braxmaier, et al. "MAQRO–BPS 2023 research campaign whitepaper" (2022).

[52] Scott Aaronson, Yosi Atia, and Leonard Susskind. "On the hardness of detecting macroscopic superpositions" (2020).

[53] E. Knill. "Approximation by quantum circuits" (1995). arXiv:quant-ph/9508006.

[54] Andreas Bärtschi and Stephan Eidenbenz. "Deterministic preparation of Dicke states". In International Symposium on Fundamentals of Computation Theory. Pages 126–139. Springer (2019).

[55] Frank Arute, Kunal Arya, Ryan Babbush, Dave Bacon, Joseph C Bardin, Rami Barends, Rupak Biswas, Sergio Boixo, Fernando GSL Brandao, David A Buell, et al. "Quantum supremacy using a programmable superconducting processor". Nature **574**, 505–510 (2019).

[56] Andrea Mari. "Counting collisions in random circuit sampling for benchmarking quantum computers" (2023).

[57] Scott Aaronson and Yuxuan Zhang. "On verifiable quantum advantage with peaked circuit sampling" (2024).

[58] Ben W Reichardt, Falk Unger, and Umesh Vazirani. "Classical command of quantum systems". Nature **496**, 456–460 (2013).

[59] Ivan Šupić and Joseph Bowles. "Self-testing of quantum systems: A review". Quantum **4**, 337 (2020).

[60] Ulysse Chabaud, Frédéric Grosshans, Elham Kashefi, and Damian Markham. "Efficient verification of boson sampling". Quantum **5**, 578 (2021).

[61] "Quantinuum H1-1". August 20-22, 2024.

[62] Stephanie Wehner, David Elkouss, and Ronald Hanson. "Quantum internet: A vision for the road ahead". Science **362**, eaam9288 (2018).

[63] Karen Wintersperger, Florian Dommert, Thomas Ehmer, Andrey Hoursanov, Johannes Klepsch, Wolfgang Mauerer, Georg Reuber, Thomas Strohm, Ming Yin, and Sebastian Luber. "Neutral atom quantum computing hardware: Performance and end-user perspective". EPJ Quantum Technology **10**, 32 (2023).

[64] Loïc Henriet, Lucas Beguin, Adrien Signoles, Thierry Lahaye, Antoine Browaeys, Georges-Olivier Reymond, and Christophe Jurczak. "Quantum computing with neutral atoms". Quantum **4**, 327 (2020).

[65] Marissa Giustina, Marijn AM Versteegh, Sören Wengerowsky, Johannes Handsteiner, Armin Hochrainer, Kevin Phelan, Fabian Steinlechner, Johannes Kofler, Jan-Åke Larsson, Carlos Abellán, et al. "Significant-loophole-free test of Bell's theorem with entangled photons". Physical review letters **115**, 250401 (2015).

[66] UnitaryFoundation. "UnitaryFoundation Research". https://github.com/unitaryfoundation/research/ (2024).

[67] "Quantinuum TKET". https://tket.quantinuum.com/. Accessed: 2024-09-03.

[68] "Quantinuum Nexus" (2024).

A Derivation of Semi-Brukner inequality without Debbie

We want to prove the inequality

$$S := -\langle A_1 B_2\rangle + \langle A_1 B_3\rangle - \langle A_3 B_2\rangle - \langle A_3 B_3\rangle \leq 2, \tag{25}$$

is obeyed when the assumptions of Absoluteness of Observed Events and Local Agency are assumed. Assuming AOE and LA implies that the distribution of outcomes a, b for Alice and Bob given measurements choices x and y respectively implies (See Sec 2.3):

$$\phi(ab|xy) = \begin{cases} \sum_c \delta_{a,c} P(b|cy)P(c) & \text{if } x = 1 \\ \sum_c P(ab|cxy)P(c) & \text{if } x \neq 1 \end{cases} \tag{26}$$

where $a, b, c \in \{-1, 1\}$, $\langle A_x B_y\rangle := \sum_{a,b} ab\phi(ab|xy)$. Expanding each term in the expression for S using the correlations defined above

$$S = \sum_c P(c)\left[-c\langle B_2\rangle_c + c\langle B_3\rangle_c - \langle A_3 B_2\rangle_c - \langle A_3 B_3\rangle_c\right] \tag{27}$$

where we define $\langle B_y\rangle_c = \sum_b bP(b|cy)$ and $\langle A_x B_y\rangle_c = \sum_c abP(ab|cxy)$. Let

$$X(c) = -c\langle B_2\rangle_c + c\langle B_3\rangle_c - \langle A_3 B_2\rangle_c - \langle A_3 B_3\rangle_c. \tag{28}$$

If we can show that $X(c) \leq 2$ for all $c \in \{-1, 1\}$, then $S \leq \sum_c P(c) \cdot 2 = 2$, since $\sum_c P(c) = 1$. Since $P(b|cy) = \sum_a P(ab|cxy)$ we have that $X(c)$ can be written as

$$X(c) = c\sum_{a,b} bP(ab|c\,3\,3) - c\sum_{a,b} bP(ab|c\,3\,2) - \sum_{a,b} abP(ab|c\,3\,2) - \sum_{a,b} abP(ab|c\,3\,3). \tag{29}$$

Here we use that the marginal $P(b|cy)$ is independent of x using the Local Agency assumptions (Sec 2.3). Rearranging the terms based on the (xy) settings for $P(ab|cxy)$:

$$X(c) = \sum_{a,b} b(c-a)P(ab|c\,3\,3) - \sum_{a,b} b(c+a)P(ab|c\,3\,2). \tag{30}$$

Now analyze the terms $c-a$ and $c+a$. Since $a, c \in \{-1, 1\}$, $X(c)$ will only be maximized when both $(c-a)$ and $(c+a)$ are non-zero:

- $c - a$ is non-zero only if $a = -c$. In this case, $c - a = c - (-c) = 2c$.
- $c + a$ is non-zero only if $a = c$. In this case, $c + a = c + c = 2c$.

Thus $X(c)$ can be maximized by setting $(c-a) = (c+a) = 2c$. The expression for $X(c)$ then simplifies to:

$$X(c) = 2c\left[\sum_b bP(a = -c, b|c\,3\,3) - \sum_b bP(a = c, b|c\,3\,2)\right]. \tag{31}$$

Let $S_1(c) = \sum_b bP(a = -c, b|c\,3\,3)$ and $S_2(c) = \sum_b bP(a = c, b|c\,3\,2)$. Then,

$$X(c) = 2c(S_1(c) - S_2(c)). \tag{32}$$

Using the triangle inequality, we have

$$|S_1(c)| \leq \sum_b P(a = -c, b|c\,3\,3) = P(a = -c|c\,3\,3).$$

Similarly, $|S_2(c)| \leq P(a = c|c\,3\,2)$. Since $|c| = 1$, again by the triangle inequality:

$$X(c) \leq 2|S_1(c) - S_2(c)| \leq 2(|S_1(c)| + |S_2(c)|). \tag{33}$$

Using the bounds for $|S_1(c)|$ and $|S_2(c)|$:

$$X(c) \leq 2\left[P(a = -c|c\,3\,3) + P(a = c|c\,3\,2)\right]. \tag{34}$$

Local Agency implies that Alice's marginal probability $P(a|cx)$ (obtained by summing $P(ab|cxy)$ over b) is independent of Bob's setting y. So, $P(a = -c|c\,3\,3) = P(a = -c|c\,3)$ and $P(a = c|c\,3\,2) = P(a = c|c\,3)$. Thus,

$$X(c) \leq 2\left[P(a = -c|c\,3) + P(a = c|c\,3)\right]. \tag{35}$$

Since a can only take values c or $-c$ (because $a, c \in \{-1, 1\}$), the sum of these probabilities is $P(a = -c|c\,3) + P(a = c|c\,3) = 1$. Therefore, $X(c) \leq 2 \cdot 1 = 2$.

Since $X(c) \leq 2$ for all possible values of c, and $P(c)$ is a probability distribution, we have:

$$S = \sum_c P(c)X(c) \leq \sum_c P(c) \cdot 2 = 2. \tag{36}$$

B Running EWFS on quantum hardware

To run the EWFS circuit on a hardware backend, the circuit must be transpiled to target the hardware architecture. Transpiling the circuit in Qiskit is achieved via the `transpile` function. This function takes an optionally specified `optimization_level` argument on how much optimization to perform on the circuit. This value equals 1 by default (with a maximum value of 3 and a minimum of 0), in which the value of 1 applies a light optimization across the overall circuit. As the `optimization_level` argument increases, more aggressive strategies are applied to the circuit via transpilation to reduce gates in the circuit and optimally route qubit mappings. In our case, we wish to avoid gate-collapsing optimizations and instead focus on ideal routing. To achieve this, we set `optimization_level=0` to avoid any gate reductions. All software used to conduct experiments, generate plot figures, and process data from both hardware and simulator devices is available on GitHub [66].

B.1 Running EWFS on IBM quantum hardware

We hand-optimize a routing layout position for the virtual qubits and physical device qubits. We perform this by supplying an argument of `initial_layout` to the `transpile` method. We construct the layout pattern based on the hardware coupling map and opt for attaining a chain-like connectivity of qubits for Alice, Bob, Charlie, and Debbie. An example of such a layout construction on the `ibm_torino` device is shown in Figure 14, but the same layout orientation strategy was followed for the other IBM hardware devices as well. As an additional step in our transpilation pipeline, we optimize single-qubit gate decompositions using the `Optimize1qGatesDecomposition` class via the `PassManager` in Qiskit.

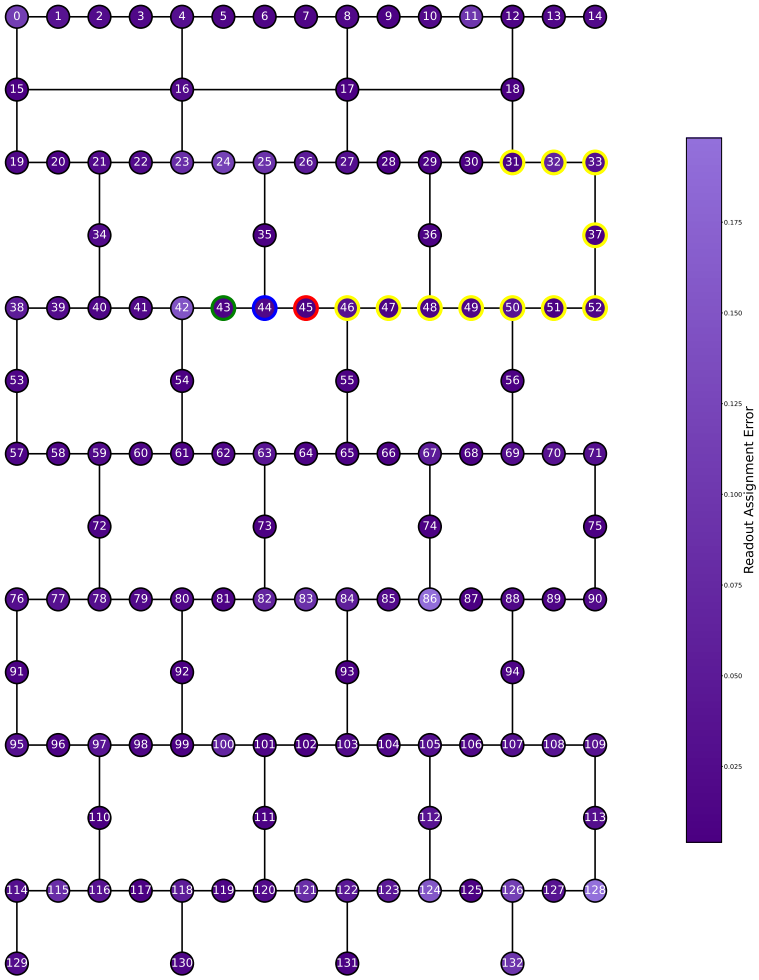

Figure 14: The calibrations coupling map for the CNOT readout error of CNOT gates for the `ibm_torino` device. Lighter colors indicate a higher CNOT error, while darker shades indicate a lower CNOT error. When targeting this device, we aim to maintain a chain-like orientation for our initial layout and also pick a layout that optimizes for the lowest readout error. Specifically, we assign nodes labeled 43 to Debbie (highlighted in green), 45 to Alice (highlighted in red), and 44 to Bob (highlighted in blue). The remaining nodes [46, 47, 48, 49, 50, 51, 52, 37, 33, 32, 31] (highlighted in yellow)represent the size of Charlie's system for progressively higher qubit systems. The nodes with the outer layer highlight indicate the qubit layout used for our experiments. This image was produced with device readout assignment error data obtained via the IBM Quantum Platform on 8-3-2024.

B.2 Running EWFS on Quantinuum H1-1 quantum hardware

Unlike the IBM hardware we target, the routing optimizations do not need to be considered, as the H1-1 device coupling map corresponds to a fully connected 20-node complete graph. This means there is no need to hand-optimize an optimal routing layout since every node is connected to every other node. We encoded our EWFS circuits in Qiskit (as we did for IBM hardware) and transpiled these circuits using TKET [67] to target the Quantinuum H1 architecture. To run our experiments, we used the Nexus [68] platform.